LARGE EDDY SIMULATION OF A LOW SPEED, HIGH ASPECT RATIO RECTANGULAR JET IN A CROSS FLOW

François Golanski, Andrew Pollard
Computational and Experimental Fluid Dynamic Laboratory,
Department of Materials and Mechanical Engineering,
Queen's University - Kingston - ON - Canada

Kevin Hall
Department of Civil Engineering
Queen's University - Kingston - ON - Canada

ABSTRACT

The modification to the structure of a high aspect ratio jet that laterally infiltrates into the cross flow of a river is considered. This jet in cross-flow configuration is different to that usually considered in the literature due to the large (50:1, long side is parallel to the main cross flow direction) aspect ratio of the side-wall jet, which can be thought of as a large underground fissure or fracture. The cross flow river flow is considered to have no zero-slip surfaces except for the plane from which the side jet issues. Two large eddy simulations are performed to ascertain grid dependency effects on the mean flow field, the instantaneous vorticity fields, and turbulence statistics. The paper also considers the transition mechanisms associated with the interaction between the low velocity side jet as it encounters the higher velocity cross-flow.

INTRODUCTION

The environmental impact of contaminant transport in rivers is an emerging major issue with possible negative impact on the local habitats. The literature on modelling the flow in rivers is extensive; however, there are apparently no publications on the application of large eddy simulation methods to investigate the detailed turbulence structures associated with the infiltration of groundwater from large aspect ratio fractures into a river flow. In this paper, the modification to the structure of a high aspect ratio jet that laterally infiltrates into the cross flow of a river is considered.

Jets-in-cross flow have been extensively studied. The basic configurations include round, elliptic, square and rectangular jets issuing into either a boundary layer, pipe or channel cross-flow, (Yuan et al. (1999); New et al. (2003); Plesniak and Cusano (2005)) In the case of rectangular jets, the major axis is typically aligned normal to the direction of the cross-flow mean velocity; and, if aligned parallel with the cross-flow mean velocity, the aspect ratio of the jet is normally less than 10:1 or so. Additionally, the ratio of the jet to cross flow mean momentum is typically greater that unity. A comprehensive review of works before 1993 can be found in Margason (1993).

In this paper, the structure of the turbulence in a weak high aspect ratio jet as it issues into a river-like cross flow (velocity ratio of 0.1) is highlighted.

FLOW PARAMETERS

The flow configuration is described in the figure 1. The basic flow arrangement is a "low" velocity rectangular jet of maximum initial velocity U_{jet}, which emerges from a solid wall and issues into a mean flow, which is oriented normal to the jet axis. The jet is modeled by a double hyperbolic tangent profile in the inflow plane (O, y, z) with a ratio $\Delta_z/\theta = 20$, where θ is the momentum boundary layer thickness at the exit of the nozzle of the jet; note that the nozzle is not considered in the present simulation. A uniform mean cross-flow V_0 in the y direction is imposed at the inflow plane π_0. The velocity ratio between the cross flow and the jet is $U_{jet}/V_0 = 0.1$. This velocity ratio, while considered relatively large by the environmental fluid dynamics community, is a starting point for the current work. This ratio will be decreased in future reports on this preliminary work. The dimensions of the jet are $\Delta_y \times \Delta_z = 50 \times 1$, and the dimensions of the whole simulation domain are $L_x \times L_y \times L_z = 10 \times 70 \times 16$. In the z-direction, the domain is thus 10 times the jet width, whereas in the y-direction, the domain is 1.4 times longer than the jet. The Reynolds number, based on the jet width Δ_z and the mean flow velocity V_0 is $Re_{\Delta_z} = 1000$.

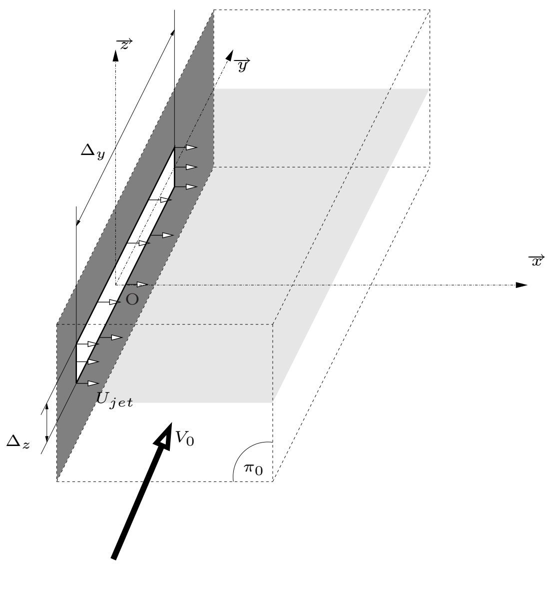

Figure 1: Flow configuration

NUMERICAL METHOD

The problem is modeled by a DNS/LES finite volume code Pierce (2001) and only the main features are provided here. The spatial discretization is performed by a second-order finite-volume method where the velocity components are staggered with respect to pressure in both space and time, which ensures a kinetic energy conservation. The time integration is similar to the Crank-Nicholson scheme but the right-hand-sides are evaluated using variables that have been interpolated in time to the midpoint between the solution at times t^n and t^{n+1}. The Poisson equation is solved by a 2D multi-grid method in each (x, y) plane whereas the z-direction is treated in the Fourier space. The sub-grid scale modeling is based on the dynamic approach of Germano et al. (1991). The grid is non-uniform, with clustering of the grid increasing inversely with distance from the wall.

Dirichlet conditions are applied on velocity components at the inflow planes. A modified outflow convective boundary conditions is applied at the outlet (Fournier et al. (2007)). Briefly, the classical convective outflow condition

$$\frac{\partial u_i}{\partial t} + U_c \frac{\partial u_i}{\partial x} = 0 \tag{1}$$

is replaced by a modified condition

$$\frac{\partial u_i}{\partial t} + u \frac{\partial u_i}{\partial x} + v \frac{\partial u_i}{\partial y} - \nu \frac{\partial^2 u_i}{\partial y^2} = 0 \tag{2}$$

This modified condition is used here to reduce the error introduced by the classical outflow convective boundary conditions when used for flows with steep gradients of the mean flow (like normal velocity in boundary layers). Periodicity is imposed in the $z-$direction.

GRID RESOLUTION EFFECTS

As mentioned above, the present configuration is unusual, and thus a grid resolution effects study was considered. Two LES simulations are presented here: a "low resolution" case with $512 \times 128 \times 256$ control volumes and a "high resolution" case with $1024 \times 256 \times 256$ control volumes. There is no *a priori* knowledge of the smallest scales to be resolved for this flow, and thus the "high resolution" case is not the preferred DNS approach, rather LES. It is thought that doubling the grid resolution from 16.7 million to 67.1 million control volumes would at least achieve results where the SGS model should not interfere with resolving the major scales of the flow. The authors continue to explore what is required to fully resolve all scales to confirm DNS resolution. In what follows, the effect of grid resolution is explored on the structural features of the jet.

Vorticity structures

The figures presented below consider the vorticity magnitude within the jet fluid as it enters the cross flow.

Figures 2 and 3 are snapshots of the vorticity norm respectively for the low and high resolution cases.

The structures formation are very similar on these two simulations. Particularly, the formation of rings all along the jet exit (fig. 2-(c) and 3-(c)) is really grid independent, and can then be considered as a particular feature of this flow. Indeed, the appearance of these structures cannot be related to any external forcing since no perturbation of any kind has been applied to these simulations.

Mean Flow

(a)

(b)

(c)

(d)

(e)

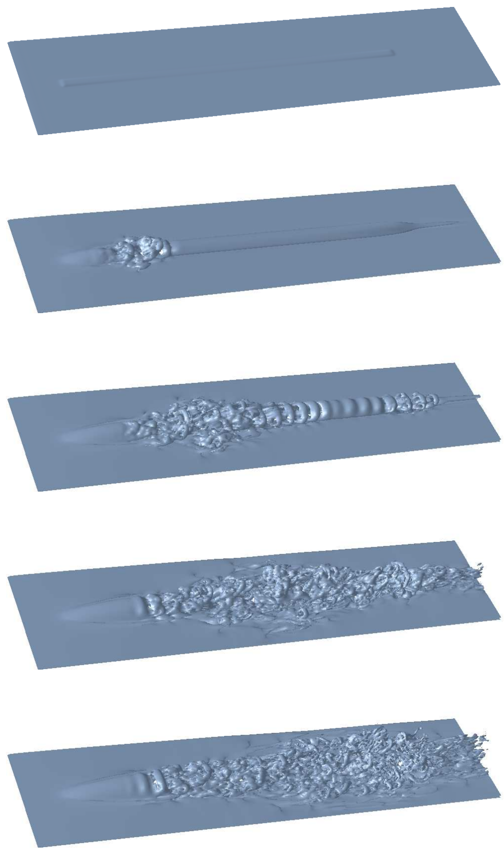

Figure 2: Vorticity norm iso-surfaces $\omega = 1.5V_0/\Delta_z$ at 5 instants (t=00, 20, 40, 60 and 80 Δ_z/V_0) for the **low resolution case**.

Figure (4) shows iso-contours of mean velocities in the plane (O, x, y) (gray plane on figure 1). In all the statistical results presented here, statistics were gathered during $T \simeq 250\Delta_z/V_0$, from $t_0 \simeq 100\Delta_z/V_0$ (which corresponds to the time needed to the first perturbations to reach the outlet). During this period of time, statistics are computed every time steps.

Very good agreement is observed between the two simulations, on $\langle u \rangle$ and $\langle v \rangle$. While a less quantitative agreement is found on $\langle w \rangle$, the region where the mean flow is actually three dimensional is the same on the two simulations.

Turbulence intensities and turbulence kinetic energy

Figure (5) shows iso-contours of turbulence intensities (noted here u', v' and w') in the plane (O, x, y) (gray plane on figure 1).

Figure (6) shows iso-contours of turbulence kinetic energy k in the plane (O, x, y) (gray plane on figure 1).

As well as for the mean flow velocities, good agreement is found for the turbulence intensities and for turbulence kinetic energy. In particular it is observed that the production of turbulent fluctuation starts at the end of the bubble region located at the junction between the main flow and the jet ($y \in [-25; -10]$ in figure 4).

Conclusion on grid resolution study

From the grid independence study, it is concluded that,

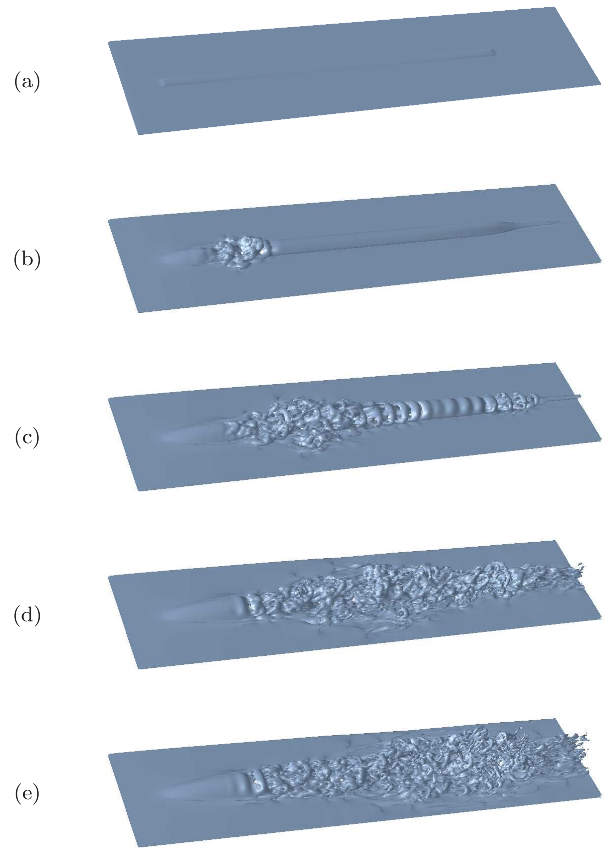

Figure 3: Vorticity norm iso-surfaces $\omega = 1.5V_0/\Delta_z$ at 5 instants (t=00, 20, 40, 60 and 80 Δ_z/V_0) for the **high resolution case**.

for the most part, the coarse resolution simulations have captured most of the features of the jet as it emerges into the cross-flow. However, the finer grid simulations provides subtle details that could be important. These data continue to be generated and analysed and will be presented more completely at the meeting.

TRANSITION MECHANISMS

As mentioned above, the main flow (in the y-direction) and the inflow-jet are laminar and in particular, no forcing or turbulent perturbation of any kind are used in these simulation. The observed vortical features are deemed inherent to the topology of this flow.

Figure 7 shows the vorticity norm in the plane (O, x, y) (gray plane on figure 1).

This figure shows that this flow can partially be seen as a quasi circular mixing layer moved from the wall by the jet. Then the main instability mechanism is very similar to the Kelvin-Helmholtz instability (with vortex creation that can be seen in fig. 7-(a) and 7-(b)). This confirms the observation already made about turbulence quantities that develop at the end of the initial "bubble". This feature is common to the more classical jet in cross-flow where the jet to cross-flow velocity ratio is higher than one. These vortices have been called the "shear layer vortices" by Fric and Roshko (1994). To support this comparison, a visualization from Fric and Roshko (1994) is provided n figure 8.

In figure 7-(d), we can observe that Kelvin-Helmholtz

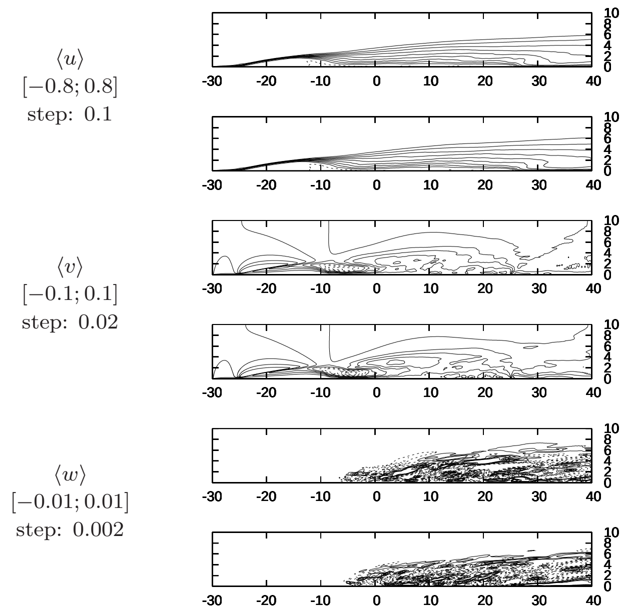

Figure 4: Iso-contours of the mean velocities in the plane (O, x, y) (for each quantity, Top: low resolution; Bottom: high resolution)

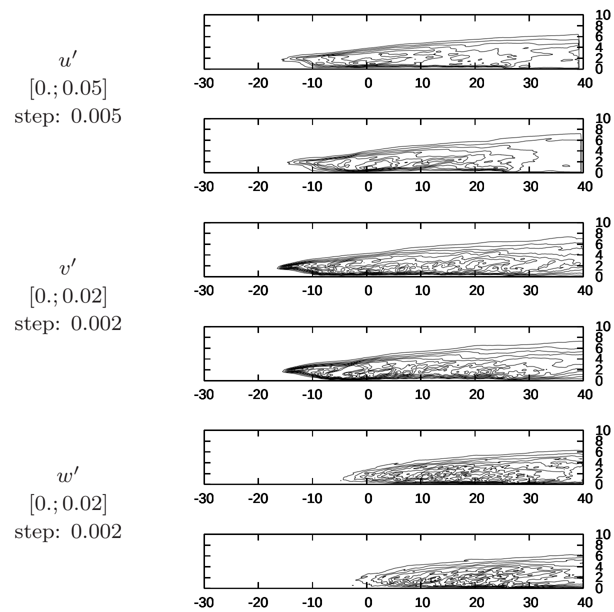

Figure 5: Iso-contours of the turbulence intensities in the plane (O, x, y) (for each quantity, Top: low resolution; Bottom: high resolution)

instability also creates vortices further downstream. These vortices could also transition to turbulence by themselves, but figure 7-(e) shows that they are immersed in the turbulence created upstream. The vortices generated at the leading edge of the jet-cross-flow interface appear to have an "knock-on" effect with upstream vortices providing a perturbation for those downstream. The authors continue to explore and quantify this effect through spectral analysis and the results will be reported later.

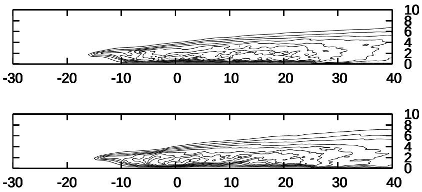

Figure 6: Iso-contours of the turbulence kinetic energy in the plane (O, x, y) (Top: low resolution; Bottom: high resolution)

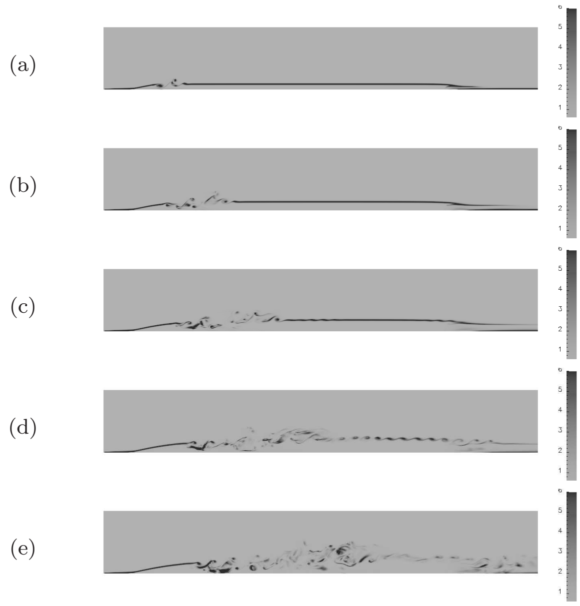

Figure 7: Vorticity norm (unit is V_0/Δ_z) at 5 instants (t=10, 20, 30, 40 and 50 Δ_z/V_0) for the high resolution case.

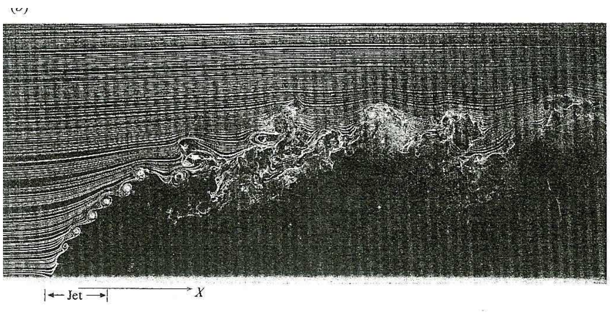

Figure 8: Visualization showing the shear layer vortices issued from the jet exit (from Fric and Roshko (1994)).

CONCLUSION

This preliminary investigation of a novel jet-in-cross-flow arrangement has revealed a number of phenomena that are believed novel; however, further study is required. First, the transition mechanisms present very interesting three-dimensional vortex coupling that require deeper analysis. Second, the influence of the free surface of the cross on the turbulence development would be of major importance and its implementation is ongoing.

ACKNOWLEDGMENTS

The authors acknowledge the Ontario Research and Development Challenge Fund for financial support and the computational resources of the High Performance Computing Virtual Laboratory. The computer code was generously supplied by the Centre for Turbulence Research, Stanford University.

*

References

G. Fournier, F. Golanski, and A. Pollard. A novel outflow boundary conditions for laminar flows. In *AERO7, Toronto, Canada, April 24-26*, 2007.

T. F. Fric and A. Roshko. Vortical structure in the wake of a transverse jet. *J. Fluid Mech.*, 279:1–47, 1994.

M. Germano, U. Piomelli, P. Moin, and H. Cabot. A dynamic subgrid-scale eddy viscosity model. *Phys. Fluids A*, 3(7):1760–1765, 1991.

R. J. Margason. Fifty years of jet in crossflow research. Technical report, AGARD-CP-534, 1993.

T. H. New, T. T. Lim, and S. C. Luo. Elliptic jets in crossflow. *J. Fluid Mech.*, 494:119–140, 2003.

C. Pierce. *Progress-variable approach for large-eddy simulation of turbulent combustion.* PhD thesis, Stanford University, June 2001.

M. W. Plesniak and D. M. Cusano. Scalar mixing in a confined rectangular jet in crossflow. *J. Fluid Mech.*, 524: 1–45, 2005.

L. L. Yuan, R. L. Street, and J. H. Ferziger. Large-eddy simulations of a round jet in crossflow. *J. Fluid Mech.*, 379:71–104, 1999.